Underwater optical wireless communications: depth dependent variations in attenuation

Laura J. Johnson,* Roger J. Green, and Mark S. Leeson

School of Engineering, Warwick University, Coventry CV4 7AL, UK

*Corresponding author: laura.j.johnson@warwick.ac.uk

Received 16 August 2013; accepted 16 October 2013;
posted 21 October 2013 (Doc. ID 195883); published 12 November 2013

Depth variations in the attenuation coefficient for light in the ocean were calculated using a one-parameter model based on the chlorophyll-a concentration C_c and experimentally-determined Gaussian chlorophyll-depth profiles. The depth profiles were related to surface chlorophyll levels for the range 0–4 mg/m^2, representing clear, open ocean. The depth where C_c became negligible was calculated to be shallower for places of high surface chlorophyll; 111.5 m for surface chlorophyll $0.8 < C_c < 2.2$ mg/m^3 compared with 415.5 m for surface $C_c < 0.04$ mg/m^3. Below this depth is the absolute minimum attenuation for underwater ocean communication links, calculated to be 0.0092 m^{-1} at a wavelength of 430 nm. By combining this with satellite surface-chlorophyll data, it is possible to quantify the attenuation between any two locations in the ocean, with applications for low-noise or secure underwater communications and vertical links from the ocean surface.

OCIS codes: (060.0060) Fiber optics and optical communications; (060.4510) Optical communications; (010.4450) Oceanic optics.

http://dx.doi.org/10.1364/AO.52.007867

1. Introduction

There is a growing interest in the use of optical wireless communications for underwater applications such as ocean monitoring and defense. Recent research has shown this technology to be capable of supporting links with up to 5 Mbps for 200 m in deep oceans [1]. A problem with this study, and a number of similar studies [2–4], is the lack of clarity about if and how the attenuation of light is changed throughout the communication link. Typically, the attenuation coefficient $c(\mathrm{m}^{-1})$, which dictates at what distance the transmitting source becomes indistinguishable, is assumed to be a constant value throughout the link. While this may be an accurate approximation for a link that is parallel to the ocean's surface, the composition of the ocean changes significantly with depth, meaning the attenuation of a vertical link is very unlikely to follow the same approximation.

The purpose of this study is to investigate how the ocean composition affects the magnitude of attenuation for communication links which have a vertical component. Using this knowledge, some of the studies that investigate underwater communication links will be reassessed. There will also be a discussion on the selection and use of appropriate wavelengths for different link orientations.

2. Background and Related Work

In order to determine how depth-varying ocean properties change the attenuation, it is necessary to first fully define attenuation by its constituent optical components. A one-parameter model [5] will then be used to show the attenuation changes in terms of a single constituent.

A. Absorption and Scattering Models

The two major causes of light attenuation underwater are scattering, where electromagnetic radiation is

1559-128X/13/337867-07$15.00/0

redirected away from its original path, and absorption, where the energy of the electromagnetic radiation is converted into another form, such as heat or chemical. Both of these processes are wavelength dependent, hence:

$$c(\lambda) = a(\lambda) + b(\lambda), \tag{1}$$

where a and b are absorption and scattering, respectively, measured m^{-1}, and λ is the vacuum wavelength of light, in nm. Using the attenuation coefficient, Beer's law determines the attenuation of an optical signal for a distance d:

$$I = I_0 e^{-c(\lambda)d}. \tag{2}$$

The form of the absorption and scattering spectra are a result of different biological factors; typically, these are grouped by their optical behaviors. For absorption, these factors include: the absorption of pure water and absorption by chlorophyll-a, which is the main substance that comprises phytoplankton, a group of photosynthesizing microorganisms, and absorption by humic and fulvic acids, both of which act as nutrients for phytoplankton. The full absorption spectrum is an addition of these spectra multiplied by their respective concentrations, such that [5]:

$$a(\lambda) = a_w(\lambda) + a_f^0 C_f \exp(-k_f\lambda) + a_h^0 C_h \exp(-k_h\lambda) + a_c^0(\lambda)(C_c/C_c^0)^{0.602}, \tag{3}$$

where a_w is the pure water absorption coefficient m^{-1}; a_f^0 is specific absorption coefficient of fulvic acid ($a_f^0 = 35.959\ m^2/mg$); a_h^0 is the specific absorption coefficient of humic acid ($a_h^0 = 18.828\ m^2/mg$); a_c^0 is the specific absorption coefficient of chlorophyll in m^{-1}; C_f is the concentration of fulvic acid in mg/m^3; C_h is the concentration of humic acid in mg/m^3; C_c is the concentration of chlorophyll-a in mg/m^3 ($C_c^0 = 1\ mg/m^3$); k_f is the fulvic acid exponential coefficient ($k_f = 0.0189\ nm^{-1}$), and k_h is the humic acid exponential coefficient ($k_h = 0.01105\ nm^{-1}$). The absorption spectra of pure water and the specific absorption spectra of chlorophyll-a have been plotted in Figs. 1(a) and 1(b), respectively, for the range $400\ nm < \lambda < 700\ nm$. In the blue–green region, absorption by pure sea water is minimal; however, this increases dramatically toward the yellow–red end of the spectrum. Conversely, the absorption of chlorophyll peaks in the blue–green region and again in the red region, but lies at a minimum for yellow wavelengths. In the clearest oceans, the total absorption by pure water is much more significant than that of chlorophyll due to the reduced concentration of chlorophyll. At concentrations of roughly $2\ mg/m^3$ or higher, chlorophyll becomes the dominant absorption

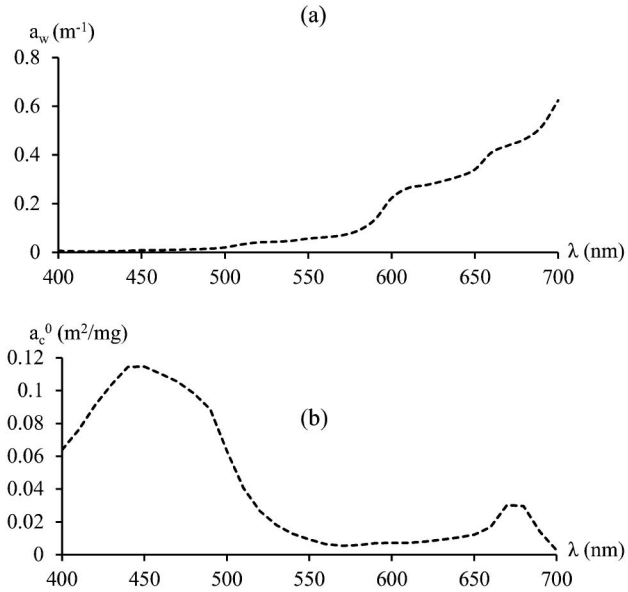

Fig. 1. Absorption spectrum for the range $400\ nm < \lambda < 700\ nm$ of (a) pure water and (b) typical profile for specific absorption by chlorophyll (calculated at the ocean surface, where $C_c < 0.04\ mg/m^2$).

mechanism, particularly for wavelengths <500 nm. Note that the values of pure water absorption are from [6] and specific chlorophyll-a absorption are calculated using the following relation, which is typical in open surface conditions:

$$a_c^0(\lambda) = A(\lambda) C_c^{-B(\lambda)}, \tag{4}$$

where A and B represent empirical constants, a full list of which is given in [7]. Such a relationship is explained by the absorption spectra of pure water and specific concentration-dependent variations in the chlorophyll pigment composition, which leads to an increased specific absorption at lower chlorophyll concentrations.

The scattering spectra are influenced by two biological factors: scattered by pure water and scattering by particulate substances. The latter is separated into small and large particles, each with a different statistical distribution and scattering strength. The full equation is given as [5]:

$$b(\lambda) = b_w(\lambda) + b_s^0(\lambda) C_s + b_l^0(\lambda) C_l, \tag{5}$$

where b_w is the pure water scattering coefficient in m^{-1}; b_s^0 is the scattering coefficient for small particulate matter in m^2/g; b_l^0 is the scattering coefficient for large particulate matter in m^2/g; C_s is the concentration of small particles in g/m^3, and C_l is the concentration of large particles in g/m^3. The spectral dependencies for the scattering coefficients of small and large particulate matter are given by the following equations:

$$b_w(\lambda) = 0.005826(400/\lambda)^{4.322}, \tag{6}$$

$$b_s^0(\lambda) = 1.1513(400/\lambda)^{1.7}, \quad (7)$$

$$b_l^0(\lambda) = 0.3411(400/\lambda)^{0.3}. \quad (8)$$

Scattering contributes much less to the overall attenuation coefficient than absorption, though it is much greater in particulate-rich areas.

B. One-Parameter Attenuation Model

Haltrin determined a one-parameter model for attenuation that simplifies equations (3) and (5) by finding the relationship between the concentrations of different particulates [1]. These concentrations were determined numerically in terms of the chlorophyll concentration to be:

$$C_f = 1.74098C_c \exp(0.12327C_c), \quad (9)$$

$$C_h = 0.19334C_c \exp(0.12343C_c), \quad (10)$$

$$C_s = 0.01739C_c \exp(0.11631C_c), \quad (11)$$

$$C_l = 0.76284C_c \exp(0.03092C_c). \quad (12)$$

Thus, if the chlorophyll concentration at any location in the ocean is known, the scattering and absorption coefficients may be calculated. The next section, therefore, looks at the distribution of chlorophyll in the ocean.

C. Chlorophyll Distribution

Chlorophyll-a is the main substance that comprises a group of microscopic organisms known as phytoplankton. As phytoplankton are photosynthesizing organisms, they inhabit only those parts of the ocean where sunlight can propagate, known as the photic or euphotic zone. Another condition for photosynthesis is the sufficiency of nutrients, which are generally more available in coastal areas due to surface-run off from land and upwelling of subsurface water into the photic zone [8]. The near-surface chlorophyll concentration of the ocean is monitored regularly by the NASA SeaWiFS (Sea-viewing Wide Field-of-view Sensor) project, which uses observation and quantification of ocean color to determine concentration [9]. Higher chlorophyll concentrations are observed along the equator, on the coastlines (specifically those that are east-facing), and in the high latitude ocean. Typical chlorophyll concentrations for the open-ocean fall within the range 0.01–4.0 mg/m^3, whereas near-shore levels may be up to 60 mg/m^3.

The chlorophyll-concentration depth profile has been investigated thoroughly due to its applications in biological productivity of the ocean. Below the photic zone, lower levels of sunlight limit the extent of photosynthesis and, therefore, reduce the chlorophyll concentration. However, nearer the surface it is the availability of nutrients that determines the chlorophyll concentration. Between these regions of sunlit, nutrient-poor water and dark, nutrient-rich water occurs the deep chlorophyll maximum (DCM)—a peak in chlorophyll concentration due to an optimal balance of light and nutrients and occurring at a depth typically between 20 and 120 m, depending on the surface concentration of chlorophyll [10].

The chlorophyll profile over a depth $z(m)$ from the surface can be modeled as a Gaussian curve that includes five numerically determined parameters, the generic form of which is [11]:

$$C_c(z) = B_0 + \mathrm{S}z + \frac{h}{\sigma\sqrt{2\pi}} \exp\left[\frac{-(z - z_{\max})^2}{2\sigma^2}\right], \quad (13)$$

where B_0 is the background chlorophyll concentration on the surface, S is the vertical gradient of concentration, which is always negative due to the slow decrease in chlorophyll concentration with depth, h is the total chlorophyll above the background levels, and $z_{\max}$ is the depth of the DCM. The standard deviation of chlorophyll concentration σ is calculated using:

$$\sigma = \frac{h}{\sqrt{2\pi[C_{\mathrm{chl}}(z_{\max}) - B_0 - \mathrm{S}z_{\max}]}}. \quad (14)$$

A difficulty arises in determining the value of these parameters because, for each surface concentration of chlorophyll, the profile shape alters. However, a study was done that quantified the parameters experimentally using 2419 separate chlorophyll profiles [12]. Ocean locations were allocated to one of nine groups, each representing a different range of surface chlorophyll concentrations. These were $<$0.04 mg/m^3, 0.04–0.08 mg/m^3, 0.08–0.12 mg/m^3, 0.12–0.2 mg/m^3, 0.2–0.3 mg/m^3, 0.3–0.4 mg/m^3, 0.4–0.8 mg/m^3, 0.8–2.2 mg/m^3, and 2.2–4 mg/m^3, represented by S1–S9, respectively. A full list of the parameters for each of these concentration ranges is given in Appendix A. There is one additional condition which must be satisfied in order for the body of water to fit these profiles; the water must be stratified so that the photic zone is smaller than the mixed layer. In the mixed layer, turbulence generated by surface conditions ensures there are no step changes in the ocean parameters, such as temperature and salinity.

The chlorophyll profiles for S1–S4 and S5–S9 have been plotted in Figs. 2(a) and 2(b), respectively. For areas with a low surface chlorophyll concentration, the chlorophyll concentration can be up to 0.3 mg/m^3 and the DCM occurs between 60 and 120 m. It should be noted that phytoplankton growth around the DCM in fact intercepts the nutrient supply in deeper waters. For this reason, the DCM is not only a response to the depth structure of nutrients and light but actually helps to set these conditions. Conversely, in areas of high surface chlorophyll

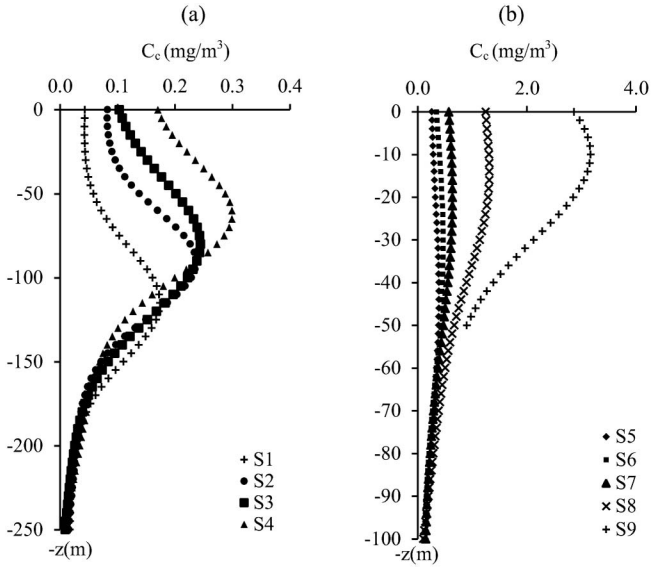

Fig. 2. Chlorophyll-concentration depth profiles for different ranges of surface chlorophyll levels, where (a) is S1–S4, and (b) is S5–S9. Definitions of S1–S9 are given in Appendix A.

concentration, the DCM appears at a depth between 10 and 40 m. This is because in these areas, the high chlorophyll level at the surface limits the depth that sunlight can penetrate, reducing the number of phytoplankton and, therefore, the chlorophyll levels in deeper waters [8]. Effectively, the chlorophyll concentration is self-limiting, where a high concentration near the surface leads to a lower concentration at a shallower depth and a high concentration lower down, at the DCM, limits the nutrients available below. The significance of these chlorophyll profiles for an underwater communication link shall be discussed in Section 3, where the relationship between the attenuation coefficient and chlorophyll concentration is determined fully. However, it is the general trend for areas with a lower chlorophyll concentration to have a lower attenuation. A significant question arises from this; what is the minimum amount of chlorophyll concentration expected? Moreover, for what range of z is Eq. (13) valid? The latter of these questions is important because, if z becomes suitably large, then the chlorophyll concentration takes a negative value, which is a physical impossibility.

To address the first question, measured values of deep-ocean chlorophyll levels from different studies were taken into account, as [12] only discusses the chlorophyll ranges given in Fig. 2. Cullen measured chlorophyll concentrations from the surface to depths of 200 m, even for areas of high surface concentration, and recorded a minimum concentration between $0 < C_c < 0.025$ mg/m^3 [13]. Cochlan *et al.* showed that at even greater depths, down to 900 m, the chlorophyll level became indistinguishable from zero [14]. Therefore, it appears that, in the deep-ocean, chlorophyll concentrations tend toward zero, meaning that there is no phytoplankton present. Biologically, this is a sensible suggestion, as there is no light available in the deep ocean except, perhaps, from a small amount of bioluminescence.

Using the assumption that the chlorophyll level decays to zero, the latter question can now be answered; what is the range of z for which Eq. (13) is valid? By setting $C_c(z)$ to zero, and taking the limit as $z \to \infty$, it was determined that the upper bound limit of z, denoted z_∞, is given as:

$$z_\infty = -B_0/S, \tag{15}$$

and the lower bound of z is zero. The values of z_∞ have been included in Appendix A for S1–S8; below these depths, the chlorophyll concentration can be assumed to be negligible.

Interestingly, areas with a higher surface chlorophyll concentration fall to a negligible level higher up. This means a communication system between, for example, 150–250 m will actually perform better in an area of high surface chlorophyll. Note that the upper bound of S9 has not been included, as this is due to S being given as zero, leading to z_∞ equal to infinity. However, the expected value of z_∞ for S9 is smaller than 111.5 m, the z_∞ of S8. This disparity is likely to have occurred from a typing error for S of S9 in [12]. Even though the peak around the DCM is accurately represented by S being zero, the lack of negative gradient means it decays to a significantly different value than in the S1–S8 profiles. The equation presented here, compared with that shown in [12], appears to be accurate down to a depth of 50 m.

3. Attenuation Depth Profile

A. Chlorophyll-Dependent Attenuation

Now that the depth-dependent chlorophyll profiles have been quantified, they can be used with the chlorophyll-attenuation relationships to determine the depth-dependent attenuation of light. An assumption is made to simplify the scope of the study: the communication link of interest is in the open ocean where long-range communications (i.e., up to several hundred meters) are viable. In the open ocean, lateral changes in the absorption and scattering coefficients happen over several kilometers, so that changes across the surface of the ocean are, therefore, taken to be negligible, even in a long-range horizontal communication link, effectively removing dependency on the (x, y) coordinates across the ocean surface.

The formula for absorption and scattering, from Eqs. (3) and (5), respectively, can now be rewritten to include the depth dependency:

$$a(\lambda, z) = a_w(\lambda) + a_f^0 \exp(-k_f\lambda)C_f(z) + a_h^0 \exp(-k_h\lambda)C_h(z) + a_c^0(\lambda, z)[C_c(z)]^{0.602}, \tag{16}$$

$$b(\lambda, z) = b_w(\lambda) + b_s^0(\lambda)C_s(z) + b_l^0(\lambda)C_l(z), \quad (17)$$

where $C_f(z)$, $C_h(z)$, and $C_s(z)$, $C_l(z)$ are the depth-dependent profiles of fulvic and humic acid and small and large particles. These profiles are determined by substituting the chlorophyll profile from Eq. (13) into the Haltrin relations in Eqs. (9)–(12). Recall that the specific attenuation of chlorophyll also contained a chlorophyll concentration term; so now too has depth dependency:

$$a_c^0(\lambda, z) = A(\lambda)C_c(z)^{-B(\lambda)}. \quad (18)$$

Using Eqs. (16)–(18), it is possible to define fully the attenuation profile with varying depth and wavelength, based only on the location of the communication system. First, the appropriate S group must be selected from surface chlorophyll levels at the chosen location; these are available from SeaWiFS data sets, as mentioned in Section 2. The chlorophyll profile is then defined using the appropriate Gaussian distribution, which means the chlorophyll-dependent profiles for fulvic and humic acid, and for small and large particles, are all also known. Substituting these profiles into Eqs. (16)–(18) for the chosen range of wavelength and depth, gives the absorption and scattering coefficients, and, finally, these are combined, as in Eq. (1), to give the overall attenuation. This process was used to find the attenuation profiles for four locations in the ocean, which represented the groups S2, S4, S6, and S8, over the wavelengths 400 nm $< \lambda <$ 700 nm.

In Fig. 3, the results of the attenuation profiles for S2, S4, S6, and S8 have been plotted for varying wavelengths and depths. The relationships portrayed in these figures are mostly dominated by the absorption spectra of pure water, particularly in areas of low chlorophyll concentration, such as the entirety of the S2 profile, and other profiles for large values of z. This is due to the very distinct

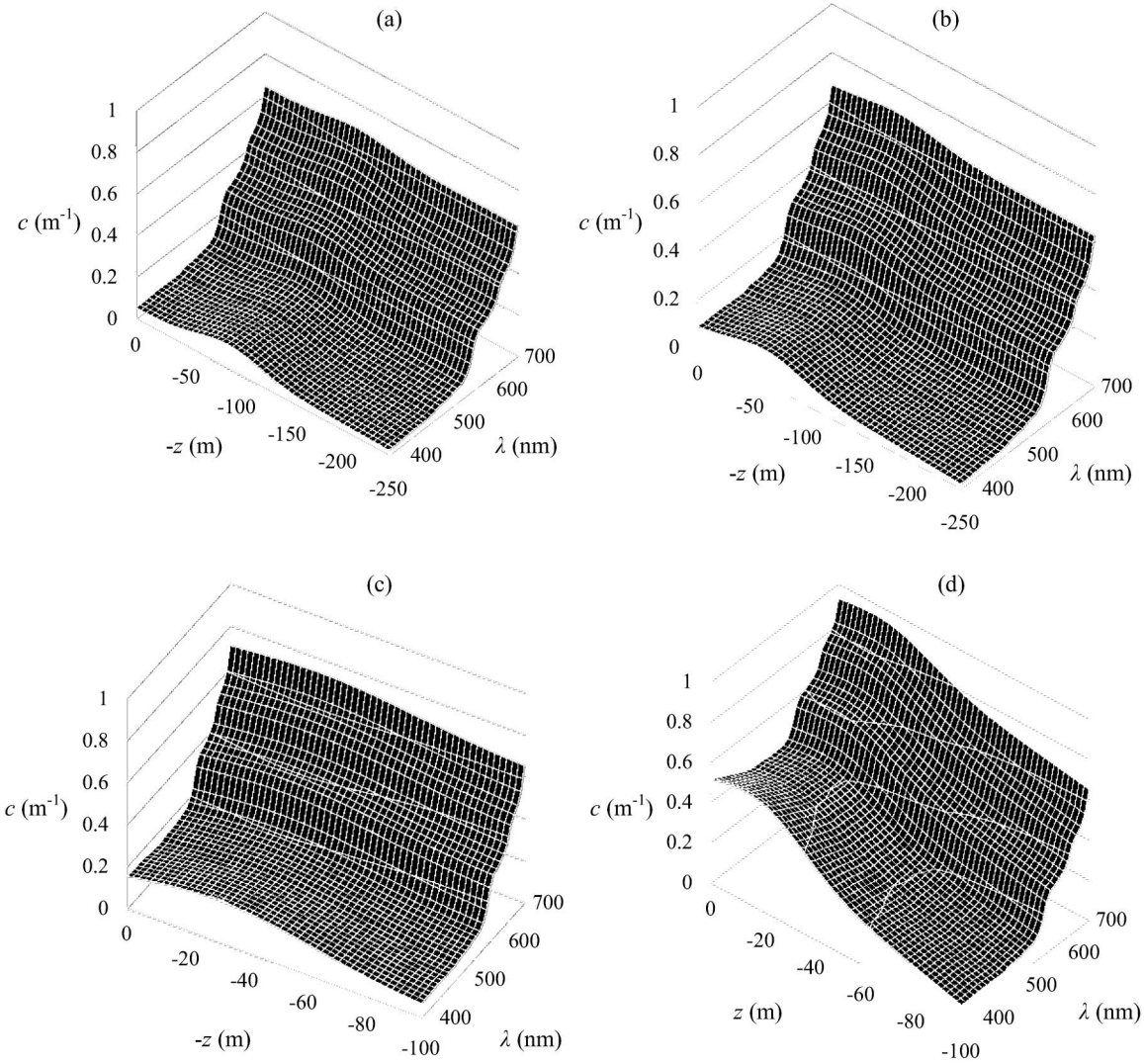

Fig. 3. Attenuation coefficient varies with wavelengths between 400 and 700 nm and depths between 0 and 250 m for (a) and (b), and 0–100 m for (c) and (d). Each subplot represents a different chlorophyll-concentration profile, each of which is based on a different range of surface chlorophyll concentrations, where (a) shows S2, which is 0.04–0.08 mg/m^3 surface chlorophyll, (b) is S4 with 0.12–0.2 mg/m^3, (c) is S6 with 0.3–0.4 mg/m^3, and (d) is for S8, representing 0.8–2.2 mg/m^3 surface chlorophyll concentration.

increase in attenuation, between 600 and 700 nm, as shown in the absorption spectra in Fig. 1(a). In areas where there is an absence of chlorophyll, the ideal wavelength of transmission becomes 430 nm, representing a deep-blue wavelength. The minimum expected attenuation coefficient is expected to be 0.0092 m^{-1}, and occurs only below the z_∞ depth (as given in Appendix A).

The main distinction between the profiles in Fig. 3 occurs due to the chlorophyll surface concentration and the location of the DCM. In the 400–500 nm range, where the attenuation profile of chlorophyll peaks [see Fig. 1(b)], the depth of the DCM is evident as it leads to a temporary increase in attenuation. For S2–S8, the DCM occurs at 90, 60, 30, and 15 m, respectively. For a communication system that is parallel to the surface and at a depth similar to the DCM, the ideal wavelength of transmission is shifted toward 500–600 nm. The ideal wavelength of a vertical optical wireless communication link for each of these profiles is extremely dependent on the expected length of the link, especially in places of high surface chlorophyll. For example, for the S8 profile, the ideal wavelength of a link between 0 and 50 m is 540 nm, whereas between 0 and 100 m this wavelength decreases to 500 nm because the chlorophyll levels reduce so rapidly at greater depth. Selection of an appropriate wavelength for a communication system depends significantly, therefore, on the expected orientation and location of the link.

B. Applications in Underwater Communications

There are two main applications within underwater communications that benefit from knowledge of the vertical profile of attenuation. The first, and most obvious, application is a communication link between a diver or autonomous vehicle at some depth, and a receiver on or above the surface. The receiver could take the form of a ship or helicopter, where the link underneath the ocean surface will be the same, though in the latter case extra consideration needs to be given to the transmission though the air and at the water/air interface. The second application is where the communication link in question needs to remain low-noise or secure.

When considering vertical communication systems between a diver and the undersurface of the ocean, the selection of a transmission wavelength is very important. This is because the wavelength that causes the minimum average attenuation can vary by as much as 100 nm, depending on the length of the link and the surface chlorophyll levels. However, for practical reasons, it is useful to choose an optimal wavelength that performs well over a range of typical depths and chlorophyll profiles. To determine this wavelength, the average attenuation coefficients for S1–S8 were recorded over links between the surface to 25, 50, 75, and 100 m. This process was repeated for all wavelengths until the optimum could be determined. The wavelength was calculated to be 490 nm, the attenuation of which varies from 0.0428 m^{-1} for S1 for a 25 m link, to 0.428 m^{-1} for S8, again for a 25 m link. These extremes show the importance of transmission depth compared to the depth of the DCM, as in the first case the communication link ends before the DCM, leading to a low overall attenuation. In the second case, the DCM occurs early in transmission, but the link length is too short to allow compensation by the more rapid decay of chlorophyll levels.

Another application of attenuation depth variation is creating low-noise underwater communications that are also secure. The idea is that the DCM will attenuate both the sunlight and any upwelling light from communication systems positioned below it. Subsequently, the link will be less affected by background light and also will not be seen from the surface. Potentially, this means higher-power lasers could be used as they will still fall within eye-safety levels at the surface. This particular application performs better in places of high surface chlorophyll, which are typical conditions for near-shore locations. In these areas, the light is attenuated more rapidly due to higher attenuation coefficient, especially if the wavelength of communication is optimized for near-pure water attenuation underneath the DCM.

C. Limitations and Future Work

In the attenuation-depth profiles calculated in this study, a small step change occurs below z_∞, where the chlorophyll concentration is assumed to be zero instead of taking the calculated negative concentration values. Time permitting, the chlorophyll-depth model could be altered to describe the chlorophyll concentration accurately for all ranges of z, omitting the step change. In the future, the chlorophyll model may be able to be extended to coastal areas that experience surface chlorophyll concentrations of up to 60 mg/m^3. However, this is currently not possible because the Haltrin relations are valid up to a chlorophyll concentration of 12 mg/m^3 only [5]. Further expansion is required on the application ideas presented in this paper, particularly for vertical communication links from an airborne craft. Ideal wavelengths in this situation would be different from the 490 nm calculated here because of the length of the link that has travelled through the air, where infrared is least attenuated. Consideration also needs to be given to what happens at the air/water interface, and whether this has a significant effect on the overall attenuation. Finally, this paper has included mainly vertical links and has not considered those which have both a horizontal and vertical component. This is because, in terms of attenuation, a vertical link is no different from a link with a vertical component. However, the refractive index of ocean water also changes with depth and potentially can lead to a long-distance communication link being diverged away from the receiver. For this reason, the study of refractive index changes with depth is an area in which ideas may be advanced further.

Appendix A: Parameter Values for S1–S9 Profiles (Table 1)

Table 1. Parameter Values for S1–S9 Chlorophyll Concentration Profiles, Where Each *S* Group is Defined by the Surface Chlorophyll Level $C_{\text{chl-surf}}$, Adapted from [12]

	$C_{\text{chl-surf}}$ (mg/m^3)	B_0 (mg/m^3)	$S(\times 10^{-3})$ (mg/m^2)	h (mg)	$z_{\max}$ (m)	$C_{\text{chl}}(z_{\max})$ (mg/m^3)	Z_∞ (m)
S1	<0.04	0.0429	−0.103	11.87	115.4	0.708	415.5
S2	0.04–0.08	0.0805	−0.260	13.89	92.01	1.055	309.6
S3	0.08–0.12	0.0792	−0.280	19.08	82.36	1.485	282.2
S4	0.12–0.2	0.143	−0.539	15.95	65.28	1.326	264.2
S5	0.2–0.3	0.207	−1.03	15.35	46.61	1.557	200.7
S6	0.3–0.4	0.160	−0.705	24.72	33.03	3.323	226.8
S7	0.4–0.8	0.329	−1.94	25.21	24.59	3.816	169.1
S8	0.8–2.2	1.01	−9.03	20.31	20.38	4.556	111.5
S9	2.2–4	0.555	0	130.6	9.87	136.5	—

The authors wish to thank the Engineering and Physical Sciences Research Council, UK, and Thales UK, for sponsorship of this work. They also wish to acknowledge the facilities provided by the School of Engineering, University of Warwick, United Kingdom.

References

1. C. Pontbriant, C. Farr, J. Ware, J. Preisig, and H. Popenoe, "Diffuse high-bandwidth optical communications," *OCEANS 2008*, September 2008, pp. 1–4.
2. M. A. Chancey, "Short range underwater optical communication links," Masters thesis (North Carolina State University, 2005).
3. J. W. Giles and I. N. Bankman, "Underwater optical communications systems. Part 2: basic design considerations," *Military Communications Conference*, October 2005, pp. 1700–1705.
4. F. Hanson and S. Radic, "High bandwidth underwater optical communication," Appl. Opt. **47**, 277–283 (2008).
5. V. I. Haltrin, "Chlorophyll-based model of seawater optical properties," Appl. Opt. **38**, 6826–6832 (1999).
6. R. M. Pope and E. S. Fry, "Absorption spectrum (380–700 nm) of pure water. II. Integrating cavity measurements," Appl. Opt. **36**, 8710–8723 (1997).
7. A. Bricaud, M. Babin, A. Morel, and H. Claustre, "Variability in the chlorophyll-specific absorption coefficients of natural phytoplankton: analysis and parameterization," J. Geophys. Res. **100**, 13321–13332 (1995).
8. D. M. Sigman and M. P. Hain, "The biological productivity of the ocean: section 1." Nat. Educ. Knowl. **3**, 21–25 (2012).
9. S. Hooker, E. Firestone, W. Esaias, G. Feldman, W. Gregg, and C. McClain, "Volume 1: an overview of SeaWiFS and ocean color," SeaWiFS Technical report series (1992).
10. J. J. Cullen, "The deep chlorophyll maximum: comparing vertical profiles of chlorophyll a" Can. J. Fish. Aquat. Sci. **39**, 791–803 (1982).
11. T. Kameda and S. Matsumura, "Chlorophyll biomass off Sanriku, Northwestern Pacific, estimated by Ocean Color and Temperature Scanner (OCTS) and a vertical distribution model," J. Oceanogr. **54**, 509–516 (1998).
12. J. Uitz, H. Claustre, A. Morel, and S. B. Hooker, "Vertical distribution of phytoplankton communities in open ocean: an assessment based on surface chlorophyll," J. Geophys. Res. **111**, C08005 (2006).
13. G. Li, Q. Lin, G. Ni, P. Shen, Y. Fan, L. Huang, and Y. Tan, "Vertical patterns of early summer chlorophyll *a* concentration in the Indian Ocean with special reference to the variation of deep chlorophyll maximum," J. Mar. Biol. **2012**, 801248 (2012).
14. W. P. Cochlan, J. Wikner, G. F. Steward, D. C. Smith, and F. Azam, "Spatial distribution of viruses, bacteria and chlorophyll a in neritic, oceanic and estuarine environments," Mar. Ecol. Prog. Ser. **92**, 77–88 (1993).